Supplementary Material

S1.1 Net Radiation

To account for any scale discrepancies between the small meteorological stations and the energy balance stations, net radiation was calculated at each small station (Brutsaert, 1982). Net shortwave radiation was calculated using the measured incoming shortwave radiation (table 1) and albedo (α) Eq. (S1):

$sw_n = (1 - \alpha) \cdot sw_i$. (S1)

Albedo was measured using solar radiometers facing up and down for 155 days between October 2011 and November 2012. Since albedo is heavily correlated with soil moisture and vegetation cover, a linear regression model of albedo based on soil moisture and NDVI was used to estimate albedo when it was not measured. When either soil moisture or NDVI was not available, a linear model based just on the other, available metric was used. Gaps were filled with a linear interpolation and data missing at the beginning of the observation were filled using a linear interpolation based on average albedo for the day of the year (between April 22-25, 2009). All estimated albedo values were smoothed using a 10-day moving average filter. Albedo fell within the acceptable range for the vegetation covers (Figure S1). Long wave radiation was calculated as the sum of long wave upwelling radiation, Eq. (S2):

$Rl_u = \varepsilon_s \sigma T_s^4$. (S2)

where ε_s is the surface emissivity, taken to have an average value (0.97), σ is the Stefan Boltzmann constant, and T_s is the measured surface temperature, and the incoming long wave radiation, which is taken as a fraction of clear sky incoming long wave radiation, Eq. (S3):

$Rl_i = Rl_{ic}(1 + am_c^b)$, (S3)

where Eq. (S4):

$Rl_{ic} = \varepsilon_{ac} \sigma T_a^4$. (S4)

and m_c is the measured cloud cover (6), a and b are constants, ε_{ac} is the atmospheric emissivity during clear sky conditions, and T_a is the measured air temperature. The atmospheric emissivity is Eq. (S5):

$\varepsilon_{ac} = a'(\frac{e_a}{T_a})^{\frac{1}{7}}$. (S5)

where e_a is the vapor pressure near the surface, determined with the measured relative humidity and air temperature and a' is calculated with a Beta function and air temperature and averages 1.24 at our site as it does for average meteorological conditions (Brutsaert, 1982). Comparison to the measured net radiation at the energy balance station (figure S2) shows some discrepancies. These may be due to the difference in wavelengths measured by the solar radiation sensors at the small meteorological stations, which use a silicon photodiode detector to detect radiation at wavelengths of 300 to 1100 nanometers. Whereas the pyranometer measures from 300 to 2800 nm and the pyrogeometer from 4.5 to 42 µm. The spectral response of the individual sensors was not available at this time, but estimation using standard spectra (ASTM G173-03 Reference Spectra) integrated over the two different short wave ranges indicates that the solar radiation sensors measure

61.78% of the energy that the pyranometers measure. These differences would be further exaggerated by the geometry of the sensor (180^o for sw_i and 150^o for sw_u from the pyranometer versus the solar radiation sensor which is less than 100% for the full 180^o) especially in dusk and dawn conditions. Additionally, the effect of albedo varies according to cloudiness and sun altitude. Most of the radiation emitted by the earth and atmosphere is between 4 and 100 µm and measurements are often flawed because instruments themselves emit radiation of comparable wavelengths and intensity to the long wave radiation that we want to measure. Thus our comparison is reasonable because it is of a similar order of magnitude, further fine-tuning the calculation will be done in a subsequent work.

References

Brutsaert, W.: Evaporation into the Atmosphere: Theory, History, and Applications, Kluwer Academic Publishers, Dordrecht, The Netherlands., 1982.

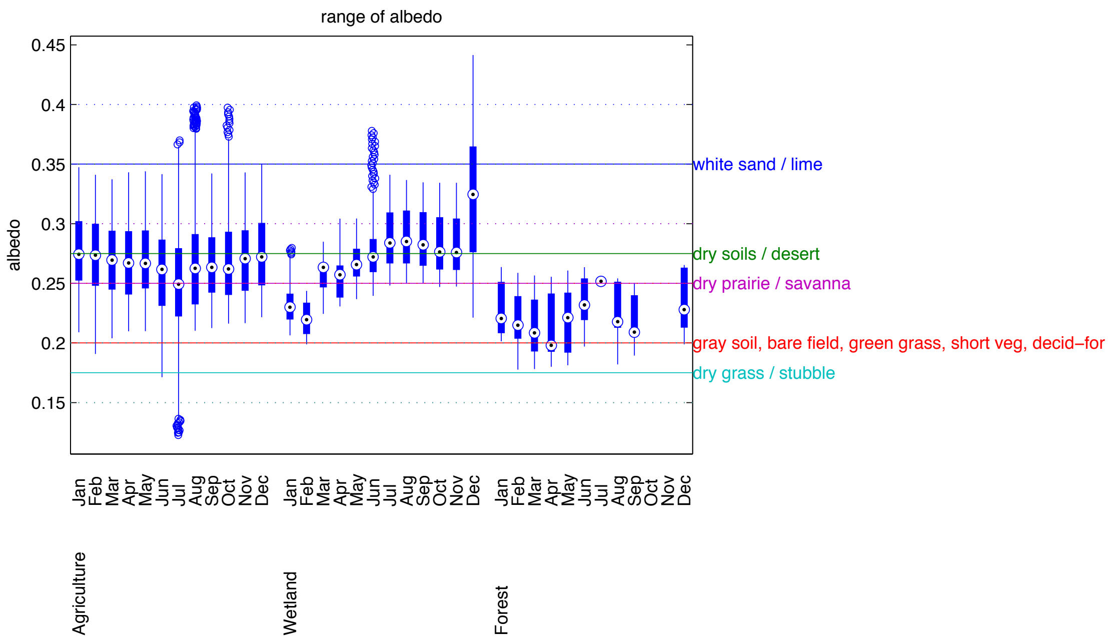

Figure S1: Distribution of albedo by landcover (Agricultural, Wetland, and Forest) and by month for the study period. The central dot is the median, the edges of the box are the 25th and 75th percentiles, the whiskers extend to the most extreme data points not considered outliers, and outliers are plotted individually. Average values for various land-covers listed by Brutsaert (1982) are drawn and labelled to the right. Ranges for these are shown in dotted lines. Our values mostly range between those of bare field or green grass and dry soils and desert, with dry prairie or savanna making a good mid value.

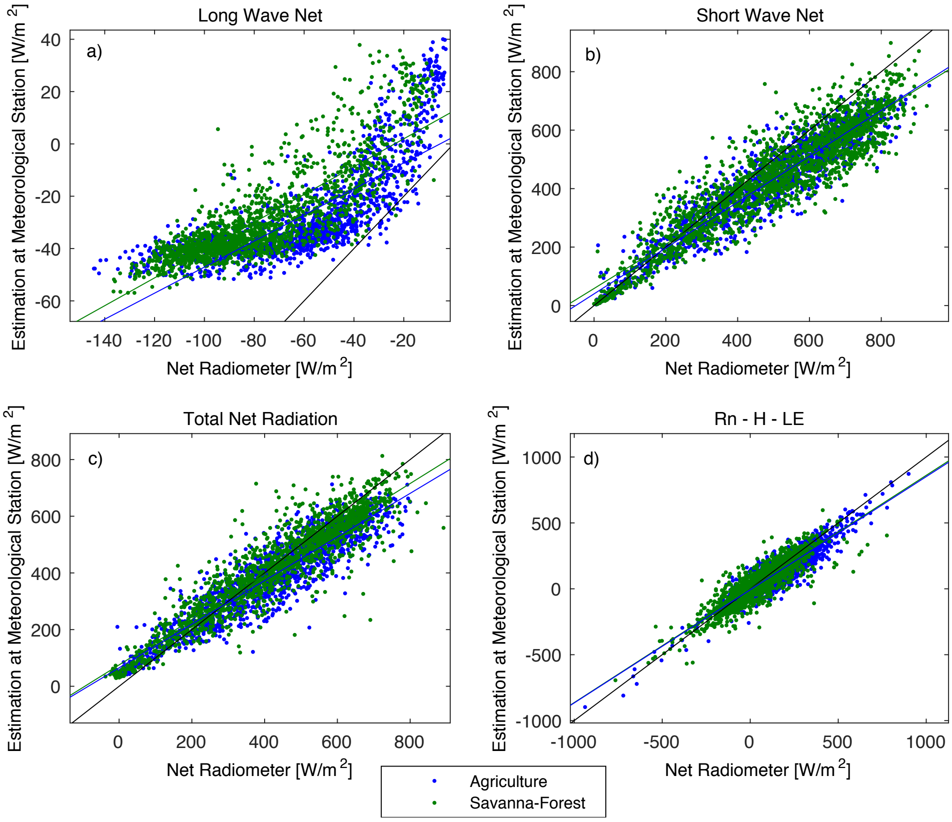

	Agriculture	Savanna-Forest
a) LW_{net}	0.58	0.50
b) SW_{net}	0.76	0.78
c) R_n	0.80	0.77
R_n -H- L_eE	0.86	0.86

Figure S2: Comparison of measurements and calculations on a half hour scale of (a) net short wave, (b) net long wave, and (c) total radiation and the residual (not shown, correlation in table) after subtracting the measured turbulent fluxes. In all cases the slope is less than 1, which means that the measurements are greater than the calculation. The slopes of the regression lines are in the accompanying table. In each plot, measurements over the agricultural field are shown in blue and over the savanna-forest are shown in green. Black lines show the one to one line and coloured lines show the least squared regression lines.

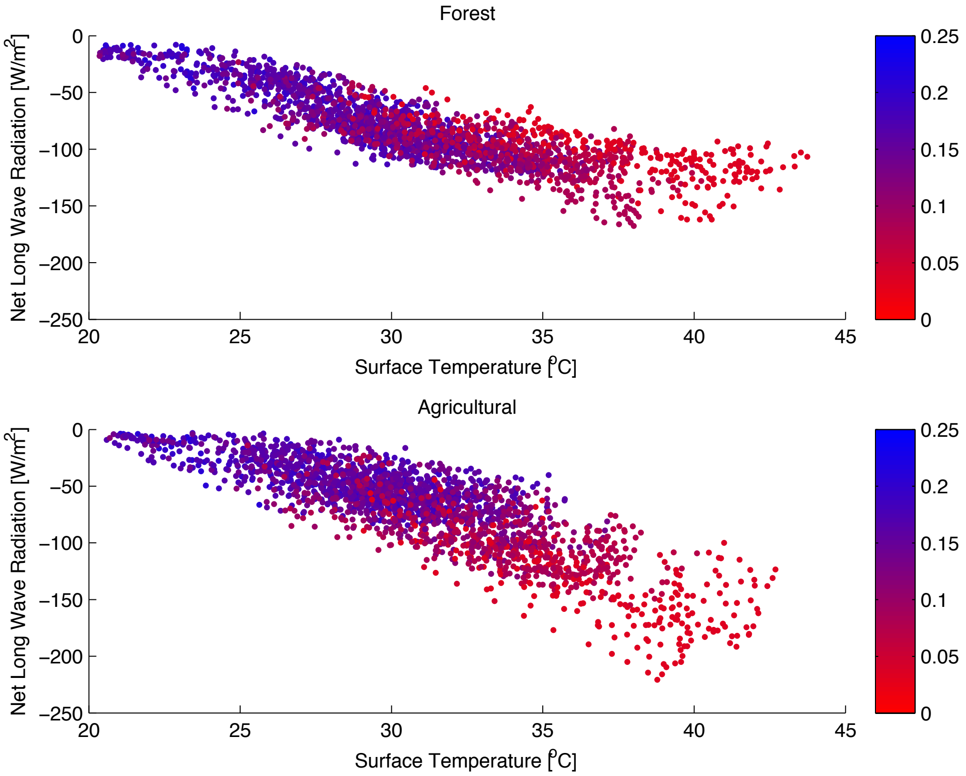

Figure S3: Net Long-wave Radiation Response to Soil Moisture and Surface Temperature. Surface temperature and net long wave radiation had a strong negative correlation with each other and also with volumetric soil water content, shown by the colour. The pattern of this correlation varied by land cover, savanna-forest above and agriculture below.